Journal of Food and Drug Analysis

Volume 25 | Issue 2 Article 8

Study on the interaction of bioactive compound S-allyl cysteine from garlic with serum albumin

Available online at www.sciencedirect.com

ScienceDirect

journal homepage: www.jfda-online.com

Original Article

Study on the interaction of bioactive compound S-allyl cysteine from garlic with serum albumin

*Yue-e Sun, Wei-dong Wang**

College of Food Engineering, Xuzhou Institute of Technology, Xuzhou 221111, China

ARTICLE INFO

Article history:
Received 28 February 2016
Received in revised form
17 August 2016
Accepted 31 August 2016
Available online 8 November 2016

Keywords:
circular dichroism
energy transfer
fluorescence quenching
human serum albumin
S-allyl cysteine

ABSTRACT

Multispectroscopic techniques were used to investigate the interaction of S-allyl cysteine (SAC) from garlic with human serum albumin (HSA). UV–Vis absorption measurements prove the formation of the HSA–SAC complex. An analysis of fluorescence spectra revealed that in the presence of SAC, the quenching mechanism of HSA is considered static. The quenching rate constant K_q, K_{SV}, and the binding constant K_A were estimated. According to the Van't Hoff equation, the thermodynamic parameters enthalpy change (ΔH) and entropy change (ΔS) were calculated to be -1.00×10^5 J/mol and -255 J/mol/K, respectively. These indicate that hydrogen bonds and van der Waals forces are the major forces between SAC and HSA. The changes in the secondary structure of HSA, which was induced by SAC, were determined by circular dichroism spectroscopy. Energy transfer was confirmed and the distance between donor and acceptor was calculated to be 2.83 nm.

1. Introduction

Serum albumin is the principal extracellular protein of the circulatory system, and accounts for about 60% of the total plasma proteins, which corresponds to a total concentration of 42 mg/mL. It provides about 80% of the colloid osmotic pressure of blood [1,2]. Human serum albumin (HSA) is the most studied serum albumin because its primary structure is well-known and its tertiary structure has been determined by X-ray crystallography. It is a single-chain, nonglycosylated globular protein consisting of 585 amino acid residues and 17 disulfide bridges that assist in maintaining its familiar heart-like shape [3]. Crystallographic data show that HSA contains three homologous a-helical domains (I, II, and III): I (residues 1–195), II (196–383), and III (384–585), each of which includes 10 helices that are divided into six-helix and four-helix subdomains (A and B). A multitude of ligand-binding sites are scattered over the entire protein. The principal regions of ligand-binding sites in HSA are located in hydrophobic cavities in subdomains IIA and IIIA, called site I and site II, respectively.

There are nine distinct fatty acid-binding sites, four thyroxine-binding sites, several metal-binding sites including albumin's N terminus, and a site centered on residue Cys34 [4]. These multiple binding sites underline the exceptional ability of HSA to act as a major depot and transport protein, capable of binding, transporting, and delivering an extraordinarily diverse range of endogenous and exogenous compounds in the bloodstream to their target organs. Many studies to date have reported on the interaction between drugs and HSA.

Garlic (*Allium sativum*) has been used historically for medicinal purposes, particularly for treatment of diseases

* *Corresponding author*. College of Food Engineering, Xuzhou Institute of Technology, No.2 Lishui Road, Xuzhou 221111, China.
E-mail address: wwd.123@163.com (W.-d. Wang).

http://dx.doi.org/10.1016/j.jfda.2016.08.013

associated with aging [5]. Aged garlic extract (AGE) possess potent antioxidant activity and is prepared from natural garlic that is aged for 20 months, which reduces its harsh irritating taste and odor. However, this aged garlic has a greater concentration of organosulfur compounds such as S-allyl cysteine (SAC), which is a potent antioxidant and free radical scavenger [6–10]. Although numerous studies have demonstrated the antioxidant properties of AGE, only limited information is available on how SAC behaves when it is absorbed and transferred in blood [11–13].

Given that SAC is the most abundant compound in AGE, this paper focuses on binding characteristics of SAC and its binding with HSA. The binding of SAC with HSA at physiological pH was evaluated using steady-state fluorescence and circular dichroism (CD) spectroscopy measurements. Results pertaining to the binding parameters, the identification of binding sites, and the nature of forces in the interaction will be beneficial for understanding the SAC metabolism.

2. Materials and methods

2.1. Materials

Fatty acid-free HSA and phosphate buffer powder were procured from Sigma (St. Louis, MO, USA). SAC (purity > 98%) was obtained from Sinopharm Co. Ltd. (Beijing, China). HSA (1×10^{-5}M) was dissolved in 0.2M phosphate buffer solution as the stock solution. Double-distilled water was used in all our experiments. All other chemicals used in this work were obtained from Tianjin Damao Chemical Corporation (Tianjin, China). Deionized water was used throughout the work.

2.2. Methods

All the fluorescence measurements were performed on Shimadzu (5301PC) spectrofluorophotometer equipped with a constant temperature holder attached with Neslab RTE-110 water bath with an accuracy of 0.1 K. Intrinsic fluorescence was measured by exciting HSA at 280 nm, and the emission spectrum was measured between 290 nm and 410 nm. The decrease in fluorescence intensity was analyzed according to the Stern–Volmer equation

$$F_0/F = 1 + K_q\tau_0[Q] = 1 + K_{SV}[Q] \quad (1)$$

where F_0 and F are the fluorescence intensities in the absence and presence of quencher (SAC), respectively; K_{SV} is the Stern–Volmer quenching constant; K_q is the bimolecular rate constant of the quenching reaction; and τ_0 is the average integral fluorescence lifetime of tryptophan (Trp), which is 5.7×10^{-9} seconds. Binding constants (K_A) and binding sites (n) were obtained using the following equation:

$$\log\frac{F_0 - F}{F} = \log K_A + n\log[Q] \quad (2)$$

where K_A is the binding constant and n is the number of binding sites.

The thermodynamic parameters were calculated to characterize the forces involved in the binding process. Because there is no significant change in temperature, enthalpy change (ΔH) can be regarded as a constant. The values of ΔH and entropy change (ΔS) can be calculated using Eq. (3) and the value of free energy change (ΔG) can be obtained using Eq. (4).

$$\ln K = -\frac{\Delta H}{RT} + \frac{\Delta S}{R} \quad (3)$$

$$\Delta G = \Delta H - T\Delta S = -RT\ln K \quad (4)$$

where K is the binding constant at corresponding temperature and R is the gas constant (8.314 J/mol/K).

The Far–UV CD spectra were measured on a Jasco-720 CD spectrophotometer (Tokyo, Japan). The CD spectra of HSA were recorded in the absence and presence of SAC using a 1-mm path length cuvette within the wavelength range of 190–240 nm. The CD results have been analyzed in terms of mean residue ellipticity in deg cm^2/dmol.

3. Results and discussion

3.1. Fluorescence quenching of HSA by SAC and binding properties

The effect of SAC on fluorescence spectra of HSA is shown in Figure 1. The excitation and emission wavelengths were 280 nm and 338 nm, respectively. The results show that the fluorescence intensity of HSA decreased with the increasing concentrations of SAC, respectively, indicating that SAC can quench the intrinsic fluorescence of HSA. The quenching rate constant of biomacromolecule (K_q) was calculated using Eq. (1). The K_q values for SAC were 5.25×10^{12} /M/s, 3.65×10^{12} /M/s, and 2.39×10^{12} /M/s at 288 K, 298 K, and 308 K, respectively (Table 1 and Figure 2). The K_q values of HSA–SAC decreased with increasing temperature, and these K_{SV} values of HSA–SAC were all far greater than the maximal collisional quenching rate constant (2×10^{10} /M/s) of all classes of the biomolecule, which suggested that fluorescent quenching between HSA and SAC was caused by static quenching rather than by dynamic collisions [14,15].

A plot of log[(F_0/F)/F] versus log[Q] and its analysis will give us the binding constant and the number of binding sites. The result indicated a good linear relationship (Figure 3), suggesting that HSA interacts with SAC in a one-to-one ratio. The binding constant was calculated from the intercept as 1.58×10^4 /M at 298 K, which indicates an adequate binding of SAC to the protein. The calculated binding constants show a comparatively weak ligand–protein interaction, compared with other strong ligand–protein complexes [16–18]. It is important to note that natural products showed binding constants, which are in the order of magnitude smaller than 10^6 /M. Other natural products such as folic acid binds with an affinity of 10^4 /M and colorant binds with an affinity of 10^5 /M [19–21].

3.2. Thermodynamic parameters and nature of binding forces

The forces acting between a compound and a biomolecule may include hydrogen bonds, van der Waals forces, hydrophobic, and electrostatic interactions. The values of thermodynamic parameters of binding reaction are the major

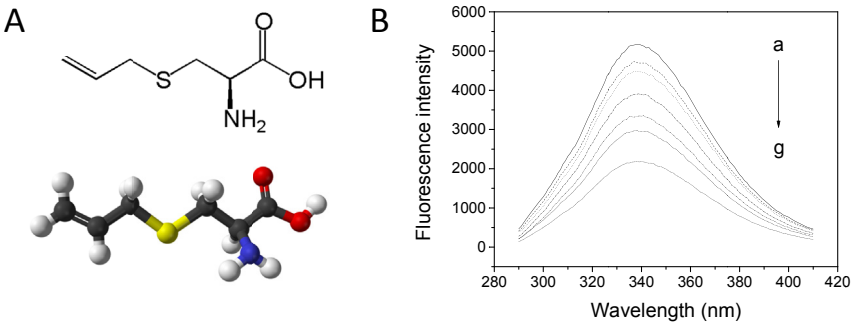

Figure 1 – (A) Molecular structure of SAC. White, yellow, red, blue, and gray represent H, S, O, N, and C, respectively. (B) Effect of SAC on the fluorescence intensity of HSA. Conditions: $T = 298$ K, pH 7.4; $c_{HSA} = 1.0 \times 10^{-6}$M; c_{SAC}: 0×10^{-6}M, 3×10^{-6}M, 5×10^{-6}M, 8×10^{-6}M, 10×10^{-6}M, 12×10^{-6}M, and 15×10^{-6}M. HSA = human serum albumin; SAC = S-allyl cysteine.

Table 1 – Stern–Volmer quenching constants, binding parameters, and thermodynamic parameters of the HSA–SAC system at different temperatures.

T (K)	Stern–Volmer quenching constants			Binding parameters			Thermodynamic parameters		
	K_q (/M/s)	K_{SV} (/M)	R	K_A (/M)	n	R	ΔG (J/mol)	ΔS (J/mol/K)	ΔH (J/mol)
288	5.25×10^{12}	5.25×10^{4}	0.9996	7.76×10^{4}	1.04	0.9993	-2.70×10^{4}		
298	3.65×10^{12}	3.65×10^{4}	0.9960	1.58×10^{4}	0.928	0.9941	-2.40×10^{4}	−255	-1.00×10^{5}
308	2.39×10^{12}	2.39×10^{4}	0.9940	5.50×10^{4}	0.867	0.9947	-2.20×10^{4}		

HSA = human serum albumin; SAC = S-allyl cysteine.

evidence for confirming the intermolecular forces. The temperatures used are 288 K, 298 K, and 308 K. The data are analyzed using Van't Hoff plot (Figure 4) and are reported in Table 1. According to the sign of ΔH and ΔS, the model of interaction between the compound and HSA can be concluded: (1) if $\Delta H > 0$ and $\Delta S > 0$, hydrophobic forces; (2) if $\Delta H < 0$ and $\Delta S < 0$, van der Waals interactions and hydrogen bonds; (3) if $\Delta H < 0$ and $\Delta S > 0$, electrostatic interactions [22–24]. Therefore, the negative ΔH and ΔS values suggest that SAC binds to HSA mainly through hydrogen bonds and van der Waals forces. The negative value of ΔG indicates that the reaction is spontaneous.

3.3. *Synchronous fluorescence spectra*

The synchronous fluorescence spectroscopy technique was introduced by Lloyd. Its spectra could provide much valuable information about the microenvironment around fluorophores in biomacromolecules. For protein molecules, when the $\Delta\lambda = 15$ nm is fixed, the spectrum characteristic of tyrosine

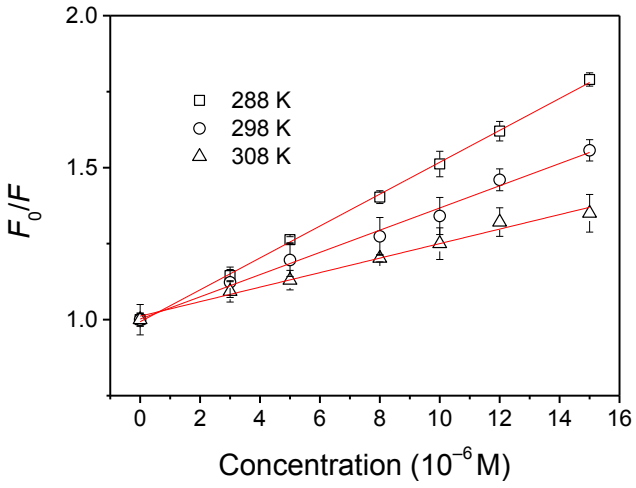

Figure 2 – Stern–Volmer plots for HSA interacting with SAC at 288 K, 298 K, and 308 K. HSA = human serum albumin; SAC = S-allyl cysteine.

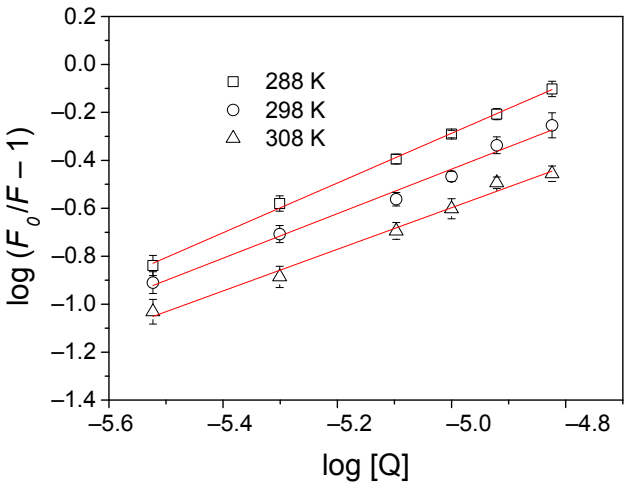

Figure 3 – Hill plots for HSA interacting with SAC at 288 K, 298 K, and 308 K. HSA = human serum albumin; SAC = S-allyl cysteine.

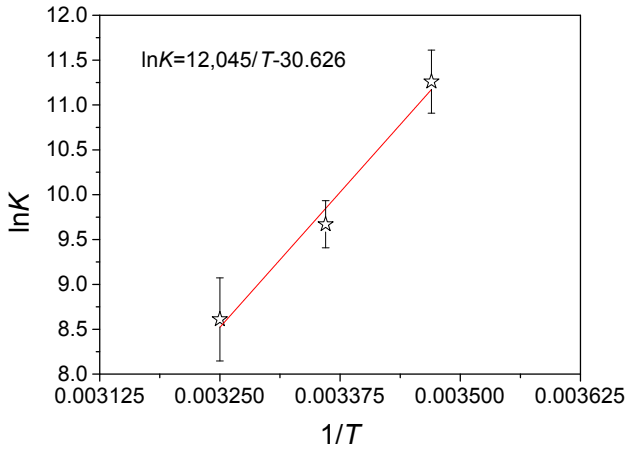

Figure 4 – Van't Hoff plot for HSA interacting with SAC at 288 K, 298 K, and 308 K. HSA = human serum albumin; SAC = S-allyl cysteine.

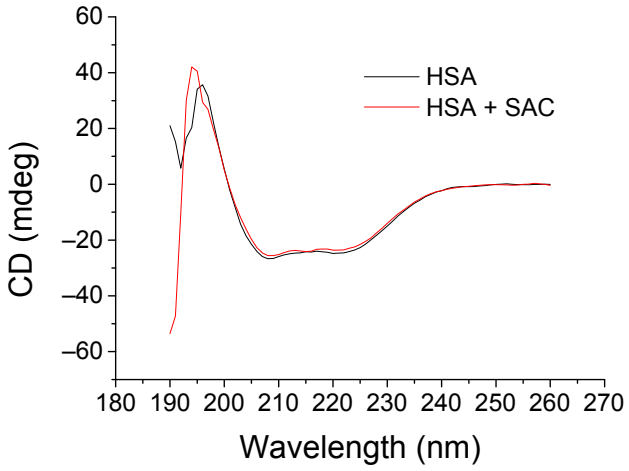

Figure 6 – Circular dichroism spectra of HSA in the absence and presence of SAC. The concentrations of HSA and SAC were 2.0×10^{-7}M and 1.0×10^{-6}M, respectively. CD = circular dichroism; HSA = human serum albumin; SAC = S-allyl cysteine.

(Tyr) residues can be observed, and when $\Delta\lambda = 60$ nm is fixed, the spectrum characteristic of Trp residues can be obtained in general [25–27]. In this study, the synchronous fluorescence spectroscopy was used to estimate the binding site of SAC to HSA molecules. From Figure 5, it can be seen that the fluorescence intensities at both $\Delta\lambda = 15$ nm and $\Delta\lambda = 60$ nm decreased gradually with the increase of SAC. A significant red shift occurred for $\Delta\lambda = 60$ nm with a maximum shift of 10 nm. This proves that SAC can bind with the Trp residues much stronger than the Tyr residues.

3.4. *Secondary structural changes of HSA upon interacting with SAC*

CD is a sensitive and useful technique to detect the conformational changes of protein induced by ligand binding. The far–UV CD profile of native HSA (Figure 6) exhibits two minima at approximately 208 nm and approximately 222 nm, which are characteristic of the α-helix-rich secondary structure (Table 2). The CD signal of HSA is found to decrease at all wavelengths with added bile salts, implying an induced perturbation of the secondary structure of the protein. A quantitative analysis of the far–UV CD spectra provides a deeper understanding of the nature of the interaction with SAC in the secondary structure of HSA. For native HSA, the α-helicity was estimated to be approximately 60%, which is in good agreement with literature reports. Addition of SAC increases the band intensity at 202 nm along with a reduction in the percentage of the α-helix from 59.4% to 52.6% and followed by an increment in random coils from 19.5% to 27.7%. Therefore, due to binding, the α-helical structure may get destroyed and a significant change over from the α-helical structure to the random structure occurs [28].

3.5. *Energy transfer from HSA to SAC*

Förster's nonradiative energy transfer theory is a distance-dependent radiation-less transfer of energy from an excited donor fluorophore to a suitable acceptor fluorophore [29,30]. The overlap between the UV spectrum of SAC and the fluorescence spectrum of HSA has been plotted in Figure 7.

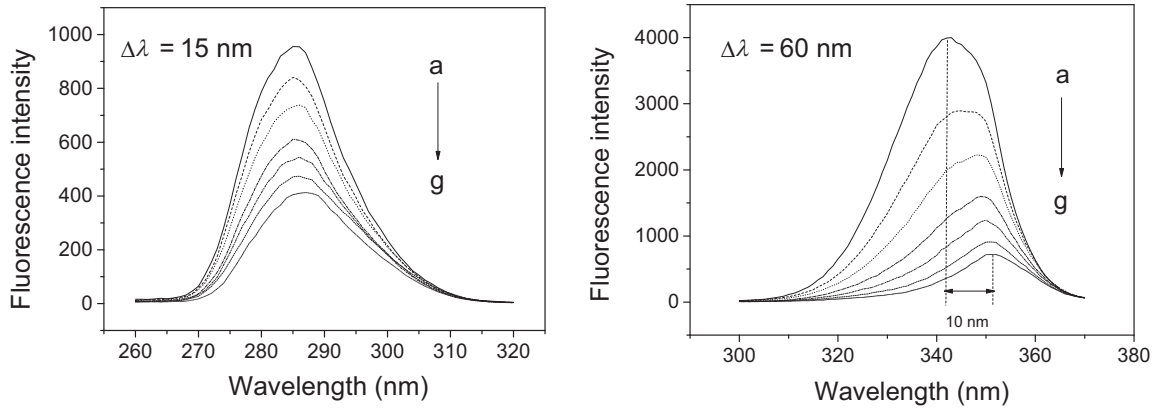

Figure 5 – Synchronous fluorescence spectra of SAC with HSA with $\Delta\lambda = 15$ nm or 60 nm at 298 K. Concentrations are consistent with the steady-state fluorescence study. HSA = human serum albumin; SAC = S-allyl cysteine.

Table 2 – Secondary structural content of HSA in the absence and presence of SAC.

Sample	Content (%)			
	α-Helix (±2%)	β-Sheet (±1%)	β-Turn (±1%)	Random coil (±2%)
HSA	59.4	10.3	10.8	19.5
HSA–SAC	52.6	10.1	9.6	27.7

HSA = human serum albumin; SAC = S-allyl cysteine.

According to Förster's nonradiative energy transfer theory, energy transfer depends on the relative orientation of the donor and acceptor dipoles, the overlapping between the absorption and fluorescence spectra of donor and acceptor, respectively, and the distance (r) between the donor and the acceptor. For an energy transfer to occur, r should be less than 8 nm. In this case, the efficiency of energy transfer (E) is given by Eq. (5)

$$E = 1 - \frac{F}{F_0} = \frac{R_0^6}{R_0^6 + r^6} \quad (5)$$

where r is the distance between acceptor (SAC) and donor (HSA) and R_0 is the critical distance when the transfer efficiency is 50%. The value for R_0 is calculated using Eqs. (5) and (6)

$$R_0^6 = 8.8 \times 10^{-25} k^2 N^{-4} \Phi J \quad (6)$$

where N is the refractive index of the medium, k^2 is the orientation factor, and Φ is the quantum yield of the donor. The spectral overlap integral (J) between the donor emission spectrum and the acceptor absorbance spectrum was approximated by the following summation:

$$J = \frac{\sum F(\lambda)\varepsilon(\lambda)\lambda^4 \Delta\lambda}{\sum F(\lambda)\Delta\lambda} \quad (7)$$

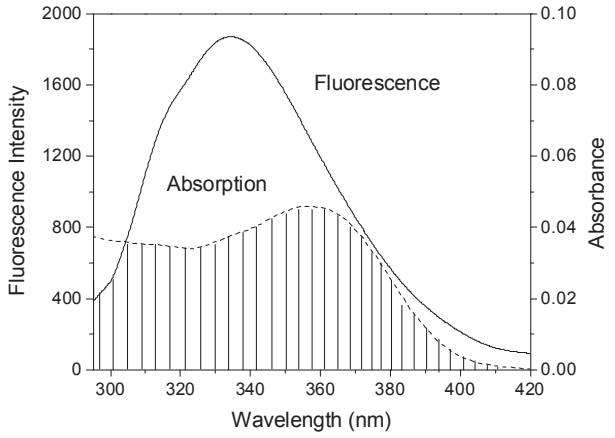

Figure 7 – The spectral overlaps of UV–Vis absorption spectra of SAC (dashed line) with the fluorescence emission spectrum of HSA (solid line). $c_{HSA} = 1.0 \times 10^{-6}$M, $c_{SAC} = 1.0 \times 10^{-6}$M, $T = 298$ K. HSA = human serum albumin; SAC = S-allyl cysteine.

where $F(\lambda)$ and $\varepsilon(\lambda)$ represent the fluorescence intensity of the donor and the molar extinction coefficient of the acceptor, respectively. From these relationships J, E, and R_0 can be calculated. For the HSA–ligand interaction, $k^2 = 2/3$, $N = 1.336$, and $\Phi = 0.15$. According to Eqs. (5)–(7), the values of the parameters were obtained as follows: $J = 2.74 \times 10^{-15}$ cm^3 L/M, $R_0 = 3.63$ nm, $E = 0.142$, and $r = 2.85$ nm. The donor-to-acceptor distance for the HSA–SAC system is less than 8 nm, and $0.5R_0 < r < 1.5R_0$, which implies high probability of energy transfer from HSA to SAC. Besides, the donor-to-acceptor distance is less than 8 nm, indicating again that the static quenching interaction occurred between HSA and SAC [31].

3.6. Conclusions

This study focused on the interaction between SAC and HSA. The stability of proteins and their interaction with other molecules is a topic of special interest in biochemistry, because many cellular processes depend on ligand binding. These interactions have immediate consequences for protein stability, as shown by the varying thermodynamic properties of the system. With a comprehensive study, we have shown that SAC quenches the fluorophore of HSA by forming ground-state complexes in solution, which, however, may get destabilized at higher temperatures. The fluorescence quenching data, analyzed by the Stern–Volmer equation, permitted us to obtain the binding stoichiometry and binding constants at different temperatures. The binding constants were calculated according to the modified Stern–Volmer equation. In particular, the calculated thermodynamic parameters suggest that binding occurs spontaneously and involves hydrogen bond and van der Waals forces, which play major roles in stabilizing the complex. The binding distance was calculated to be 2.85 nm, according to the fluorescence and UV–Vis spectral overlap. Conformational investigation from far–UV CD and FTIR also revealed that the conformation of HSA was changed in the presence of SAC. The structural alteration due to SAC supports the idea that H bonding is associated with protein structural deformation. Furthermore, the decrease of the α-helix content, at least on the structure of HSA, may ascribe to the distinct property of the water-soluble SAC. This work provides a comprehensive and basic framework for the binding mechanism of SAC with HSA and is helpful for understanding its effect on compounds transported in the biological system.

Conflicts of interest

The authors have no conflicts of interest to declare.

Acknowledgments

This work was supported by the National Natural Science Foundation of China (31301535) and Qing Lan Project.

REFERENCES

[1] Meloun B, Moravek L, Kostka V. Complete amino acid sequence of human serum albumin. FEBS Lett 1975;58:134–7.
[2] Zhao X, Lu D, Hao F, Liu R. Exploring the diameter and surface dependent conformational changes in carbon nanotube-protein corona and the related cytotoxicity. J Hazard Mater 2015;292:98–107.
[3] Koch-Weser J, Sellers EM. Binding of drugs to serum albumin. N Engl J Med 1976;294:311–6.
[4] Morgan WT, Smith A, Koskelo P. The interaction of human serum albumin and hemopexin with porphyrins. Biochim Biophys Acta 1980;624:271–85.
[5] Atif F, Yousuf S, Agrawal SK. S-allyl l-cysteine diminishes cerebral ischemia-induced mitochondrial dysfunctions in hippocampus. Brain Res 2009;1265:128–37.
[6] Welch C, Wuarin L, Sidell N. Antiproliferative effect of the garlic compound S-allyl cysteine on human neuroblastoma cells *in vitro*. Cancer Lett 1992;63:211–9.
[7] Kim KM, Chun SB, Koo MS, Choi WJ, Kim TW, Kwon YG, Chung HT, Billiar TR, Kim YM. Differential regulation of NO availability from macrophages and endothelial cells by the garlic component S-allyl cysteine. Free Radica Biol Med 2001;30:747–56.
[8] Bae SE, Cho SY, Won YD, Lee SH, Park HJ. A comparative study of the different analytical methods for analysis of S-allyl cysteine in black garlic by HPLC. LWT-Food Sci Technol 2012;46:532–5.
[9] Weerawatanakorn M, Wu JC, Pan MH, Ho CT. Reactivity and stability of selected flavor compounds. J Food Drug Anal 2015;23:179–90.
[10] Guo XK, Sun HP, Shen S, Sun Y, Xie FL, Tao L, Guo QL, Jiang C, You QD. Synthesis and evaluation of gambogic acid derivatives as antitumor agents. Part III. Chem Biodivers 2013;10:73–85.
[11] Gıtin L, Dinica R, Neagu C, Dumitrascu L. Sulfur compounds identification and quantification from *Allium* spp. fresh leaves. J Food Drug Anal 2014;30:e6.
[12] Geng Z, Rong Y, Lau BH. S-allyl cysteine inhibits activation of nuclear factor kappa B in human T cells. Free Radica Biol Med 1997;23:345–50.
[13] Kim SH, Sun Y, Kaplan JA, Grinstaff MW, Parquette JR. Photo-crosslinking of a self-assembled coumarin-dipeptide hydrogel. New J Chem 2015;39:3225–8.
[14] Zhao X, Liu R, Teng Y, Liu X. The interaction between Ag^{+} and bovine serum albumin: a spectroscopic investigation. Sci Total Environ 2011;409:892–7.
[15] Sun Y, Shieh A, Kim SH, King S, Kim A, Sun H-L, Croce CM, Parquette JR. The self-assembly of a camptothecin-lysine nanotube,. Bioorg Med Chem Lett 2016;26:2834–8.
[16] Bourassa P, Bariyanga J, Tajmir-Riahi HA. Binding sites of resveratrol, genistein and curcumin with milk α- and β-caseins. J Phys Chem B 2013;117:1287–95.
[17] Ma JY, Chen KH, Zheng XF, Guo M, Ma J, Tang Q, Wang YL, Hu JH. Spectroscopy study on the interaction of colchicine and human serum albumin. Guang Pu Xue Yu Guang Pu Fen Xi 2007;27:2485–9 [Article in Chinese].
[18] Matei I, Hillebrand M. Interaction of kaempferol with human serum albumin: a fluorescence and circular dichroism study. J Pharm Biomed Anal 2010;51:768–73.
[19] He W, Li Y, Xue C, Hu Z, Chen X, Sheng F. Effect of Chinese medicine alpinetin on the structure of human serum albumin. Bioorg Med Chem 2005;13:1837–45.
[20] Bourassa P, Hasni I, Tajmir-Riahi HA. Folic acid complexes with human and bovine serum albumins. Food Chem 2011;129:1148–55.
[21] Shahabadi N, Maghsudi M, Rouhani S. Study on the interaction of food colourant quinoline yellow with bovine serum albumin by spectroscopic techniques. Food Chem 2012;135:1836–41.
[22] Zhao XC, Liu RT, Chi ZX, Teng Y, Qin PF. New insights into the behavior of bovine serum albumin adsorbed onto carbon nanotubes: comprehensive spectroscopic studies. J Phys Chem B 2010;114:5625–31.
[23] Qian Y, Zhou X, Chen J, Zhang Y. Binding of bezafibrate to human serum albumin: insight into the non-covalent interaction of an emerging contaminant with biomacromolecules. Molecules 2012;17:6821–31.
[24] Agudelo D, Bourassa P, Bruneau J, Berube G, Asselin E, Tajmir-Riahi HA. Probing the binding sites of antibiotic drugs doxorubicin and N-(trifluoroacetyl) doxorubicin with human and bovine serum albumins. PLoS One 2012;7:13.
[25] Wu Y. Study on the interaction between salicylic acid and catalase by spectroscopic methods. J Pharm Biomed Anal 2007;44:796–801.
[26] Sun H, Zhu J, Chen Y, Sun Y, Zhi H, Li H, You Y, Xiao Q. Docking study and three-dimensional quantitative structure-activity relationship (3D-QSAR) analyses and novel molecular design of a series of 4-aminoquinazolines as inhibitors of aurora B kinase. Chin J Chem 2011;29:1785–99.
[27] Zhu S, Liu Y. Spectroscopic analyses on interaction of naphazoline hydrochloride with bovine serum albumin. Spectrochim Acta A Mol Biomol Spectrosc 2012;98:142–7.
[28] Zhao X, Hao F, Lu D, Liu W, Zhou Q, Jiang G. Influence of the surface functional group density on the carbon-nanotube-induced α-chymotrypsin structure and activity alterations. ACS Appl Mater Interfaces 2015;7:18880–90.
[29] Zhao X, Sheng F, Zheng J, Liu R. Composition and stability of anthocyanins from purple solanum tuberosum and their protective influence on Cr(VI) targeted to bovine serum albumin. J Agric Food Chem 2011;59:7902–9.
[30] Maiti TK, Ghosh KS, Samanta A, Dasgupta S. The interaction of silibinin with human serum albumin: a spectroscopic investigation. J Photochem Photobiol B 2008;194:297–307.
[31] Wu J, Wei R, Wang H, Li T, Ren W. Underlying the mechanism of vancomycin and human serum albumin interaction: a biophysical study. J Biochem Mol Toxicol 2013;27:463–70.